Vibrational spectra of multishell fullerenes

Tibor F. Nagy, Kevin J. Conley, and David Tománek

Department of Physics and Astronomy and Center for Fundamental Materials Research, Michigan State University,
East Lansing, Michigan 48824-1116

We calculate the equilibrium structure of spherical multishell fullerenes and the low-frequency rattling modes of the nested shells. The pairwise nature of the intershell interactions allows us to topologically map these zero-dimensional systems onto a linear chain of fullerene shells. Even though the masses of the individual shells and the intershell interactions depend strongly on the shell number, the vibrational density of states of very large structures resembles closely that of an infinite linear chain with site-independent masses and force constants and a very low Debye frequency of 80.2 cm^{-1}.

The recently discovered spherical multishell fullerenes[1,2] are structures consisting of nested shells of graphitic carbon, reminiscent of an onion. Systems with up to hundreds of shells have been synthesized by exposing carbon soot to an intense electron beam[1] or to thermal treatment,[3] and have subsequently been found in the mineral shungite.[4] With an intershell separation of ≈ 3.5 Å observed by transmission electron microscopy,[1] spherical multishell fullerenes are the zero-dimensional analog of graphite.

Theoretical results indicate that the absence of dangling bonds and the attractive intershell interaction makes spherical multishell fullerenes the most stable isomers of carbon clusters.[5-7] Electronic intershell coupling is likely to modestly broaden and shift the collective plasmon peak predicted and observed in free fullerenes such as the C_{60} molecule.[8-12] This collective excitation in multishell fullerenes may lie at the origin of the unexplained absorption band at 217.5 nm in the interstellar dust.[13]

The vibrational spectrum of these intriguing structures, which has not been investigated so far, is expected to be very different from that of any other known molecule. This results from a unique combination of covalent intrashell interactions, which causes the rigidity of the shells, and weak interactions which couple these shells. As we will argue in the following, the vibrational density of states of very large systems is nearly constant in the low-frequency range, reminiscent of the spectrum of a linear chain. The unusually flat vibrational absorption spectrum also suggests an exotic application of these systems as a vibrational isolation of nanostructures.

The high structural rigidity of fullerenes is reflected in the relatively hard intrashell vibrational frequencies, which for a free C_{60} molecule range from $\nu_v = 273$–1469 cm^{-1}.[14] These hard modes of the individual fullerene shells are likely to dominate the high-frequency end of the vibrational spectrum of multishell fullerenes. The intershell modes are expected to dominate the low-frequency part of the spectrum, due to the weak interaction between the shells which is derived from the interlayer bonding in graphite, and the large mass of the individual shells. Owing to the different natures of intrashell and intershell bonding, and to the vastly different vibrational frequency ranges, we expect the hybridization between intrashell and intershell modes to be negligible and the vibrational spectrum to be a superposition of the soft intershell and the hard intrashell modes. Consequently, the vibrational spectrum of multishell fullerenes can be separated into hard vibrational modes of the individual shells, and the soft intershell modes involving the rigid shells.

In the following, we will first determine the equilibrium structure — in particular, the shell radii — of spherical multishell fullerenes, and subsequently calculate their low-frequency intershell vibrational modes. Guided by the transmission electron microscopy images of these systems[1] and theoretical arguments,[5,15] we consider the individual shells to be spherical. The area per carbon atom in the shells is the same as in free fullerenes and lies close to the graphite value $A_C = 2.619$ Å^2.

Vibrational modes involving the rigid nested shells of graphitic carbon in the multishell structures are related to c-axis compression modes of graphite. As indicated in Fig. 1(a), these modes can be topologically mapped onto those of a linear chain. Our calculation of the underlying elastic interactions is based on previously published *ab initio* local-density-functional (LDA) results for graphite,[16] shown by the data points in Fig. 1(b).

In graphite, we define the elastic energy per carbon atom ΔE due to the change of the interlayer separation d as

$$\Delta E(d) = E(d) - E(d_e) , \qquad (1)$$

where $E(d_e)$ is the binding energy value at the equilibrium value of d. We use the approach of Ref. 17 and fit the long-range, partly van der Waals, interaction between atoms in neighboring layers by a modified Morse potential. As in Ref. 17, we interpolate this interaction over the dense atomic lattice to determine the interaction energy $\tilde{U}(r)$ between two small *areas* in different layers. We assume that the direct interaction between such areas is completely screened by any graphitic fragment which intercepts the direct line connecting these areas, which
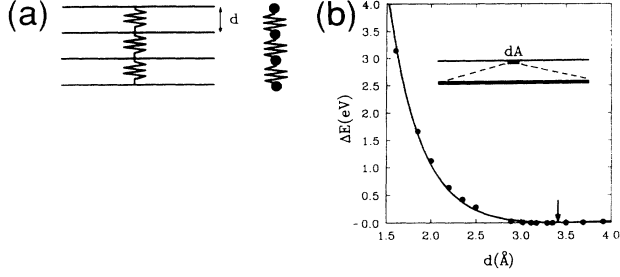
FIG. 1. Equilibrium structure and elastic behavior of graphite. (a) Schematic view of the geometry and interlayer interactions, as well as a topological mapping onto a linear chain. (b) Elastic energy ΔE of hexagonal graphite (per carbon atom, with respect to graphite layers at the equilibrium distance d_e) as a function of the interlayer spacing d. The solid line represents a modified Morse fit [Eqs. (2) and (3)] to ab initio LDA results of Ref. 16. In the inset, the infinite interaction range of the small layer area dA with the neighboring layer is symbolized by a thick line.

limits the range of interaction to adjacent graphite layers.

The interaction range of a carbon atom at $\mathbf{r}$, associated with the surface area $\Delta A = A_C$, in the adjacent graphite layer is illustrated by the inset in Fig. 1(b). The corresponding interaction energy is given by

$$E = A_C \int_{A'} d\mathbf{r}' \tilde{U}(|\mathbf{r} - \mathbf{r}'|) , \qquad (2)$$

where A' spans the neighboring layer and

$$\tilde{U}(r) = \tilde{D}_e[(1 - e^{-\alpha(r-r_e)})^2 - 1] + \tilde{E}_r e^{-\beta r} . \qquad (3)$$

The resulting elastic energy ΔE of graphite, obtained using Eqs. (1)–(3) and parameters of footnote,[18] is given by the solid line in Fig. 1(b).

As shown in Fig. 2(a), multishell fullerene structures can be topologically mapped onto a linear elastic chain in the same way as graphite. We determine the equilibrium geometry of the onion structure by minimizing the intershell interaction, given by Eq. (2). The interaction energy ΔE (with respect to its optimum value) between a fixed C_{60} shell with the radius $R_{in} = 3.55$ Å and an adjacent shell of variable radius $R_{out} = R_{in} + \Delta R$ is given in Fig. 2(b).[19] Starting with a C_{60} core shell, this procedure yields all intershell distances ΔR and shell radii R_n. As shown in Fig. 2(c), the intershell separations converge slowly from $\Delta R_1 = 3.66$ Å at the core shell towards the graphite value $\Delta R_\infty = 3.42$ Å at the surface of an infinitely large multishell fullerene.

Once the equilibrium shell sizes are determined, the shell masses can be easily obtained from the shell radii R_n, using $M_n = m_C(4\pi R_n^2/A_C)$, where m_C is the mass of a carbon atom. The mass dependence on the shell number is displayed in Fig. 3(a). Since the equilibrium intershell separation is nearly constant, R_n shows a near-linear and the shell mass M_n a near-quadratic dependence on the shell number n.

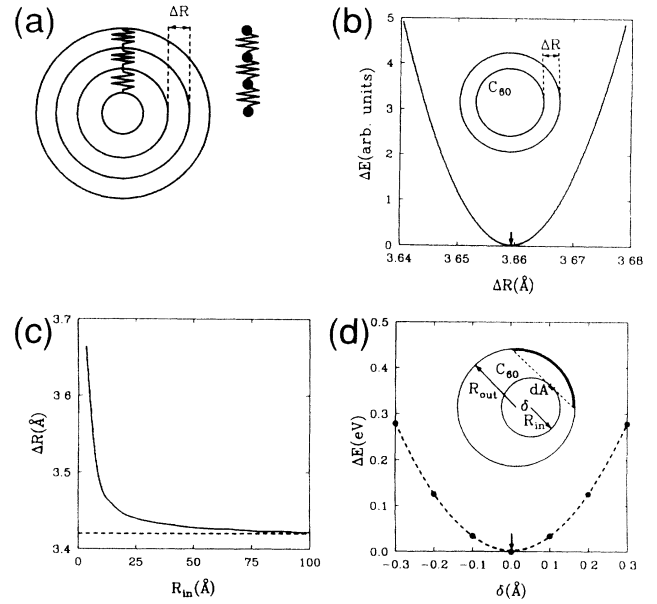With the equilibrium shell radii at hand, we proceed

FIG. 2. Equilibrium structure and elastic behavior of spherical multishell fullerenes. (a) Schematic view of the geometry and intershell interactions, as well as a topological mapping onto a linear chain. (b) Interaction energy ΔE between a spherical shell of radius $R_{in} = 3.55$ Å, corresponding to C_{60}, and a concentric spherical outer shell of radius R_{out}, as a function of $\Delta R = R_{out} - R_{in}$ (see inset). (c) Equilibrium intershell separation ΔR as a function of the inner shell radius R_{in}. (d) Elastic energy ΔE due to an off-center displacement by δ of a spherical shell with radius $R_{in} = 3.55$ Å inside a concentric spherical outer shell with radius $R_{out} = 7.21$ Å. The dashed line is the harmonic fit to the data points. The displacement geometry is given in the inset; the limited interaction range of the small shell area dA is shown by a thick line on the outer shell.

to map the elastic behavior of the spherical multishell fullerene onto a chain in three dimensions. We determine the harmonic intershell force constants from total energy differences between structures with displaced rigid shells. As mentioned above and illustrated in the inset of Fig. 2(d), a given surface area of the inner shell interacts only with a finite size cap on the outer shell. Due to the spherical symmetry of the system, the interaction between adjacent rigid shells is isotropic and only depends
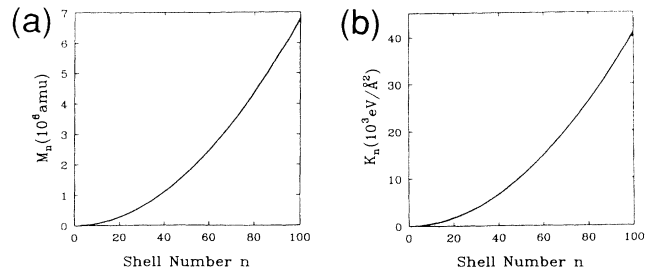

FIG. 3. (a) Shell masses M_n and (b) intershell force constants K_n as a function of the shell number n in a spherical multishell fullerene.

BRIEF REPORTS

on one parameter, the off-center displacement δ. The displacement energy $\Delta E(\delta)$ for the pair consisting of a C_{60} core shell and the adjacent shell is given in Fig. 2(d), together with the second order polynomial fit to the data points, which gives the force constant K_1. This method is used to determine all force constants K_n associated with the elastic interaction between shells n and $n+1$. The dependence of the intershell force constant K_n on the shell number is shown in Fig. 3(b). Also this quantity shows

a near-quadratic dependence on the shell number n. For shells with large n, we find $K_n/M_n \approx 5.8 \times 10^{25}$ s^{-2}.

With these masses and force constants, we determine the vibrational spectrum by calculating the eigenvalues of the mass-weighted force constant matrix V, as

$$\det \left(\mathbf{V} - \omega^2 \mathbf{I} \right) = 0. \tag{4}$$

Here, V is given in mass-weighted coordinates[20] as

$$\mathbf{V} = \begin{pmatrix} \frac{K_1}{M_1} & -\frac{K_1}{(M_1 M_2)^{1/2}} & 0 & \cdots \\ -\frac{K_1}{(M_1 M_2)^{1/2}} & \frac{K_1+K_2}{M_2} & -\frac{K_2}{(M_2 M_3)^{1/2}} & 0 \\ \vdots & 0 & -\frac{K_{n_s-1}}{(M_{n_s-1}M_{n_s})^{1/2}} & \frac{K_{n_s-1}}{M_{n_s}} \end{pmatrix}. \tag{5}$$

Due to the pairwise nature of nearest neighbor intershell interactions, V is tridiagonal. The vibration spectrum of a multishell fullerene with n_s spherical fullerene shells consists of $3n_s-3$ normal modes. Each eigenfrequency is threefold degenerate due to the fact that the three translational degrees of freedom of each spherical shell are equivalent.

The vibrational density of states $D(\nu)/n_s$ of a hypothetical spherical multishell fullerene with an infinite number of shells, normalized by the number of shells n_s, is given by the solid line in Fig. 4. Since each shell has three translational degrees of freedom, the integral $\int_0^\infty d\nu D(\nu)/n_s = 3$. For the sake of comparison, we also show the vibrational density of states of an infinite linear chain with constant masses M and pairwise force constants K in the same figure. This vibrational density of states is also likely to resemble closely that of large finite multishell fullerenes, where structural imperfections in the individual shells would split the degeneracy of the discrete vibrational modes and hence smear out the spectrum.

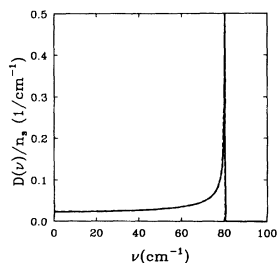As mentioned above, the physical origin of the ab-

sorption band at 217.5 nm in the interstellar dust[13] is still under discussion. Experimental observations[8,9] and calculations[10-12] for single-shell C_{60}-C_{100} fullerenes indicate that the absorption spectrum of all these structures is nearly independent of the system size or shape, and is closely related to the π-plasmon mode of graphite. In multishell systems, on the other hand, this collective mode of each shell couples to that of the neighboring shells by the depolarization field, which causes a broadening to a band.[21] This broadening is likely to be further increased due to the vibrational motion of these shells. Since the centroid position and the effective width of this absorption peak depend on the number of shells,[21] the small, yet measurable, differences in this absorption feature between different regions of interstellar space[13] may be explained by different sizes of multishell fullerenes, which are expected to develop under different synthesis conditions.

In summary, we calculated the equilibrium structure of spherical multishell fullerenes and the low-frequency rattling modes of the nested shells. We found that the pairwise nature of the intershell interactions allowed us to map topologically these zero-dimensional systems onto a linear chain of fullerene shells. Even though the masses of the individual shells and the intershell interactions depend strongly on the shell number, the vibrational density of states of very large structures was found to resemble closely that of an infinite linear chain with site-independent masses and force constants and a very low Debye frequency of 80.2 cm^{-1}.

FIG. 4. Vibrational density of states $D(\nu)$, normalized per shell, for a multishell fullerene with the number of shells $n_s \to \infty$ (solid line). For the sake of comparison, the phonon density of states for an infinite linear chain with $\nu_D = 2\sqrt{K/M} = 80.2$ cm^{-1} is given by the dashed line.

[1] D. Ugarte, Nature **359**, 707 (1992).

[2] D. Ugarte, Europhys. Lett. **22**, 45 (1993); D. Ugarte, Z. Phys. D **26**, 150 (1993).

[3] D. Ugarte, Chem. Phys. Lett. **198**, 596 (1992).

[4] T.K. Daly, P.R. Buseck, P. Williams, and C.F. Lewis, Science **259**, 1599 (1993).

[5] D. Tománek, W. Zhong, and E. Krastev, Phys. Rev. B **48**, 15 461 (1993).

[6] A. Maiti, C.J. Brabec, and J. Bernholc, Phys. Rev. Lett. **70**, 3023 (1993).

[7] D.H. Robertson, D.W. Brenner, and J.W. Mintmire, Phys. Rev. B **45**, 12 592 (1992); J.W. Mintmire, D.H. Robertson, and C.T. White, J. Phys. Chem. Solids **54**, 1835 (1993).

[8] J.W. Keller and M.A. Coplan, Chem. Phys. Lett. **193**, 89 (1992).

[9] I.V. Hertel, H. Steger, J. de Vries, B. Weisser, C. Menzel, B. Kamke, and W. Kamke, Phys. Rev. Lett. **68**, 784 (1992).

[10] G.F. Bertsch, A. Bulgac, D. Tománek, and Y. Wang, Phys. Rev. Lett. **67**, 2690 (1991).

[11] A. Bulgac and N. Ju, Phys. Rev. B **46**, 4297 (1992); Nengjiu Ju, Aurel Bulgac, and John W. Keller, *ibid.* **48**, 9071 (1993).

[12] David Tománek (unpublished).

[13] H.W. Kroto and K. McKay, Nature **331**, 328 (1988); E.L. Wright, *ibid.* **336**, 227 (1988); John S. Mathis, Rep. Prog. Phys. **56**, 605 (1993); D.G.B. Whittet, *Dust in the Galactic Environment* (Institute of Physics Publishing, Bristol, 1992).

[14] D.S. Bethune, G. Meijer, W.C. Tang, J.H. Rosen, W.G. Golden, H. Seki, C.A. Brown, and M.S. de Vries, Chem. Phys. Lett. **179**, 181 (1991).

[15] Spherical rather than faceted structure of the individual shells is expected in multishell fullerenes, since the gained intershell interaction energy at the optimum nesting geometry outweighs the energy investment to deform a faceted fullerene to a sphere.

[16] G. Overney, D. Tománek, W. Zhong, Z. Sun, H. Miyazaki, S.D. Mahanti, and H.-J. Güntherodt, J. Phys. Condens. Matter **4**, 4233 (1992).

[17] Yang Wang, D. Tománek, and G.F. Bertsch, Phys. Rev. B **44**, 6562 (1991).

[18] In Eq. (3), we use $\tilde{D}_e = 9.01 \times 10^{-4}$ eV Å^{-4}, $\alpha = 1.00$ Å^{-1}, $r_e = 4.05$ Å, $\tilde{E}_r = 164.6$ eV Å^{-4}, and $\beta = 4.0$ Å^{-1}.

[19] This procedure is consistent with, but does not necessarily imply, a growth mechanism of multishell fullerenes, where atom accretion in an incomplete shell occurs outside a closed inner shell acting as template.

[20] Mass-weighted coordinates ξ_i are introduced to symmetrize the mass-weighted force constant matrix. They are related to the displacement u_i from equilibrium by $\xi_i = M_i^{1/2} u_i$, where M_i is the mass associated with i.

[21] D. Östling, A. Rosén, P. Apell, and G. Mukhopadhyay (unpublished).